



Elliott et al.:

Toward Achieving Harmonization in a Nanocytotoxicity Assay Measurement Through an Interlaboratory Comparison Study

Supplementary Data

A Supplementary methods

Calculation of relative absorbance values

For the CdSO₄ treatment conditions, the relative absorbance values were calculated using the ratio of the absorbance values at 490 nm for the treatment condition subtracted by the no cell background values (control 1) to the absorbance value for the CdSO₄ vehicle control cells (control 7) subtracted by the no cell background values (control 1). The following are the equations used for several of the treatment conditions (Fig. 2 at <https://doi.org/10.14573/altex.1605021> shows the plate layout).

$$\text{relative absorbance (0)} = (\text{median (B3-B5)} - \text{median (B2-G2)}) / (\text{median(B3-B5)} - \text{median (B2-G2)}) = 1$$

$$\text{relative absorbance (1)} = (\text{median (C3-C5)} - \text{median (B2-G2)}) / (\text{median(B3-B5)} - \text{median (B2-G2)})$$

$$\text{relative absorbance (10)} = (\text{median (D3-D5)} - \text{median (B2-G2)}) / (\text{median(B3-B5)} - \text{median (B2-G2)})$$

$$\text{relative absorbance (25)} = (\text{median (E3-E5)} - \text{median (B2-G2)}) / (\text{median(B3-B5)} - \text{median (B2-G2)})$$

For the NP treatment conditions, the relative absorbance values were calculated using the ratio of the absorbance values at 490 nm for the treatment conditions subtracted by background (no cells but with NP addition at the treatment concentration) to the absorbance value for the NP vehicle control cells (control 8) subtracted by the no cell background. The following are the equations used for several of the treatment conditions (Fig. 2 at <https://doi.org/10.14573/altex.1605021> shows the plate layout).

$$\text{relative absorbance (0)} = (\text{median (B8-B10)} - \text{value (B11)}) / (\text{median(B8-B10)} - \text{value (B11)}) = 1$$

$$\text{relative absorbance (1)} = (\text{median (C8-C10)} - \text{value (C11)}) / (\text{median(B8-B10)} - \text{value (B11)})$$

$$\text{relative absorbance (10)} = (\text{median (D8-D10)} - \text{value (D11)}) / (\text{median(B8-B10)} - \text{value (B11)})$$

$$\text{relative absorbance (25)} = (\text{median (E8-E10)} - \text{value (E11)}) / (\text{median(B8-B10)} - \text{value (B11)})$$

In vitro sedimentation, diffusion and dosimetry modeling

The main transport processes of particles in suspension are diffusion (Stokes-Einstein Equation) and gravitational settling (Stokes' Law), both of which directly depend on particle size and density. Diffusion is inversely related to particle diameter while sedimentation is driven by particle diameter to the power of two (Teeguarden et al., 2007). Thus, the agglomeration of primary particles is a process that affects particle size, shape and density and therefore directly affects particle transport (Hinderliter et al., 2010; DeLoid et al., 2014). Typically, an agglomerate possesses interparticle pore space, i.e., entrapped media between its constituent primary particles, because the particles are not efficiently packed, which is why they have been modeled as a fractal structure (Sterling et al., 2005; Hinderliter et al., 2010). Interparticle pore space affects both agglomerate porosity and reduces the resulting agglomerate density. The two main sources of interparticle pore space in agglomerates are packing effects and the fractal nature of a particle, the former of which is described by the packing factor (PF) and the latter of which by the fractal dimension (FD), both of which are not well known and not experimentally measurable (Cohen et al., 2012). The packing factor (PF) describes how particles are packed into agglomerates and depends on the monomer shape. The value for the PF is between 0 and 1 (absence of porosity, efficiently packed), and the empiric default is 0.637 for randomly packed spherical monomers. The fractal dimension (FD) depends on how the agglomerate forms through flocculation and takes on values between 1 (rod shaped) and 3 (perfect sphere, porosity = 0), and its empiric default value is 2.3 (Cohen et al., 2012; Hinderliter et al., 2010). The ISDD model based on agglomerate diameter (i.e., using the Sterling equation) was used to estimate the effective NP dose at the plate surface in the presence



This is an Open Access article distributed under the terms of the Creative Commons Attribution 4.0 International license (<http://creativecommons.org/licenses/by/4.0/>), which permits unrestricted use, distribution and reproduction in any medium, provided the original work is appropriately cited.

<https://doi.org/10.14573/altex.1605021s>



and absence of serum in the culture media. It uses the agglomerate diameter and FD to calculate agglomerate density, porosity and transport. All of the input parameters used to model the NH₂-PS NPs in the MTS assay are listed in Table S8.

The simulation yields four output values: 1) the fraction of administered dose deposited and the corresponding 2) total number, 3) total surface area (of a sphere) [cm²] and lastly 4) total mass [μg] in terms of primary NPs deposited. These values were then normalized to the total surface area of the well bottom corresponding to the 96-well plates (0.34 cm²) to obtain the mass dose [μg/cm²], number dose [# /cm²] and surface area dose [cm² NPs/cm² well bottom], which were then used to interpret the obtained dose-response relationships and EC₅₀ values.

B Supplementary results and discussion

In vitro sedimentation, diffusion and dosimetry modeling

ISDD simulations suggest that the delivered dose at the bottom of the exposure vessel is time and treatment dependent (Tab. S6). The administered NP concentration did not affect the fraction of the delivered dose, which is in line with the underlying model assumptions that do not account for dynamic NP interactions and agglomeration during the simulated exposure period. The fraction of administered dose was highest for smallest particles and decreased with increasing diameters (Tab. S6), which may be explained by the reduced density of large agglomerates through media entrapment within, approximating that of the media itself, and also suggests that diffusion was the dominant

particle transport process. This observation is consistent with previous simulations of carboxylated polystyrene particles of similar sizes (Hinderliter et al., 2010). The fraction of administered dose delivered in the serum-free treatment at 24 h and serum treatments at 48 h was 0.1846 and 0.0662, respectively (Tab. S6); uncertainty values calculated based on changing the z-average diameter by 10% are provided in Table S6. It must be noted, however, that the ISDD model generally overestimates the deposited fraction of administered dose. In the case of carboxylated polystyrene the ratio of simulated to measured rates of transport has been shown to vary from 0.37 up to three-fold, for NP diameters 100 nm to 1100 nm (Hinderliter et al., 2010). This is likely due to the underlying model assumptions, most importantly concerning the bottom boundary condition assuming a 100% sticky well bottom (i.e., NPs that reach the bottom are immediately internalized by cells and no longer affect particokinetics) and other limitations recently described by DeLoid et al. (2015).

Dosimetrically adjusted EC₅₀ values reported in delivered dose metrics are provided in Table S7, and have important implications for the interpretation of the potency of NH₂-PS NPs as well as the biological responses. The adjusted dose metrics are similar between the two exposure conditions, suggesting that the differences implied by the conventional administered dose metric are likely due to differential particokinetics in serum-containing and serum-free conditions rather than biological activity of particles/cell sensitivity in serum-containing and serum-free conditions. These findings highlight the importance of integrating the bioavailability of NPs into *in vitro* nanotoxicity testing.

Tab. S1: Reagent supply

Lab	CdSO ₄ ¹	NP ²	Serum	Medium	Manufacturer for cell culturing containers	96-well plate plastic
EMPA	EMPA	EMPA	Lonza-Brazilian ³	Sigma-Aldrich	TPP	TPP
JRC	EMPA	EMPA	Invitrogen – New Zealand	Invitrogen – EU	BD Falcon	BD Falcon
KRISS	EMPA	EMPA	Welgene	Welgene	SPL	SPL
NANOTEC	EMPA	EMPA	Invitrogen-US	Invitrogen-US	Corning	Corning
NIST	EMPA	EMPA	Invitrogen-US	Invitrogen-US	BD Falcon	BD Falcon

¹ Hydrated CdSO₄ (97%) was dissolved in 18 MΩ water to make a 100 μM solution.

² NH₂-PS NP were purchased from Bangs as a 10 μg/ml solution in aqueous solution.

³ All serum was heat-inactivated except that used by NIST.



Tab. S2: Procedures

Lab	Harvesting	Splitting/ seeding ¹	Counting method	Cell resuspension	Washing step ²	Nanoparticle dispersion ³	Plate reader ⁴
EMPA	trypsin	3 day - 4 day Seed after 1-2-3-4 days ⁵	Hemocytometer	Rocker	Multiple vacuum aspiration	Vortex/pipette	BioTek
JRC	trypsin	3 day - 4 day Seed at split	Hemocytometer	Pipette action	Single pipette aspiration	Vortex/pipette	FLUOstar Omega (BMG Labtech)
KRISS	trypsin	2 day Seed at split	Hemocytometer	Pipette action	Single pipette aspiration	Vortex/pipette	Molecular Devices
NANOTEC	trypsin	2 day - 3 day Seed at split	CASY	Pipette action	Single pipette aspiration	Vortex/pipette	BioTek
NIST	trypsin	3 day - 4 day Seed at split	Coulter	Pipette action	Single vacuum aspiration	Vortex/pipette	BioTek

¹ Top values are the splitting cycle during routine passaging. The second value is when cells were seeded for experiment round. Cells were split at $\approx 70\%$ confluence levels and seeded at densities that resulted in 70% confluence after the desired time before the next passage. For example, with a 3-4 day passage schedule using T25 flasks, cells were seeded at 200,000 and 110,000 cells/flask or the 3 day and 4 day passage, respectively.

² Single pipette aspiration was performed with a manual micro pipette. It appears to be gentler than vacuum aspiration as determined by background absorbance measurement in the NP control experiments.

³ Vortex/pipetting refers to the procedure basically described in the protocol and in Zook et al. (2011).

⁴ All laboratories tested the repeatability of their plate reader for a single plate and measured a coefficient of variation less than 2%.

⁵ Approximately the same number of cells that were cultured for 1, 2, 3 or 4 days after splitting were combined and then seeded on the 96-well plate.

Tab. S3: Cell line characteristics

Cell line	Cell cycle time (h)	Medium volume (μm^3) ¹	Short tandem repeat (STR) analysis ²
A549-A	22.6 \pm 2.2 ³	2327 \pm 94 ³	Missing allele 12 (CSF1PO)
A549-B	22.5 \pm 2.4 ³	2047 \pm 90 ³	In agreement with ATCC

¹ from Coulter counter at passage 7

² Promega PowerPlex Fusion STR Kit

³ The values for the cell cycle time were averaged over 16 passages for each cell line, while the values for the medium volume are from three passages near the passaged used for seeding the MTS assay experiments for each cell line. The values are mean \pm standard deviation. The values for both measurements were not statistically different between the two cell lines ($p < 0.05$), two-tailed t-test.

Tab. S4: Dynamic light scattering & zeta potential of the NH₂-PS NP

Solvent	DLS (nm) ²			Zeta potential (mV)		
	0 h	24 h	48 h	0 h	24 h	48 h
De-ionized water ¹	56.6 \pm 0.9	55.9 \pm 0.9	54.5 \pm 0.9	48.8 \pm 1.9	53.4 \pm 0.8	48.9 \pm 1.4
Serum-free medium	56.7 \pm 1.0	61.8 \pm 0.8	67.5 \pm 1.3	24.5 \pm 1.4	23.5 \pm 1.2	24.1 \pm 1.7
0.1% FBS medium	1100 \pm 55	2012 \pm 80	2390 \pm 91	-0.9 \pm 0.3	-7.1 \pm 0.7	-6.8 \pm 1.1
10% FBS medium	1258 \pm 54	1126 \pm 37	1258 \pm 36	-10.7 \pm 0.9	-11.2 \pm 1.6	-11.1 \pm 1.2

¹ 18 M Ω -cm water

² All data are the mean \pm standard deviation of six measurements.

**Tab. S5: EC₅₀ values for NH₂-PS NP in A549-A and A549-B cells in the presence of serum and in serum-free conditions**

	Mean (mg/l) ¹	Median (mg/l)	95% CI (lower limit, upper limit) (µg/l)
<i>A549-A cells – serum free</i>			
Consensus	22.5	22.5	16.6, 28.5
Lab A ²	10.4	10.4	10.1, 11.1
Lab B	21.1	21.1	19.5, 22.6
Lab C	21.2	21.2	20.3, 22.1
Lab D	25.1	25.1	24, 26.4
<i>A549-B cells – serum free</i>			
Consensus	22.1	22.2	16.9, 27.2
Lab A	22.6	22.6	21, 24.4
Lab B	23.6	23.6	22.2, 24.7
Lab C	23.3	23.3	22, 24.4
Lab D	25.8	25.7	25.1, 27.4
Lab E	15.3	15.4	11.5, 18.8
<i>A549-A cells – with serum</i>			
Consensus	57.7	57.1	47.2, 71.2
Lab A	52.2	52.2	50.7, 54.0
Lab B	52.8	52.7	48.4, 58.1
Lab C	61.6	61.0	54.5, 72.8
Lab D	64.1	63.3	53.9, 79.6
<i>A549-B cells – with serum</i>			
Consensus	52.6	52.6	44.1, 62.6
Lab A	47.6	47.5	46.2, 48.7
Lab B	49.7	49.6	46.7, 52.8
Lab C	62.7	62.4	58.9, 68.0
Lab D	56.1	56.0	52.1, 61.1
Lab E	47.2	47.3	45.2, 49.2

¹ The mean, median, and 95% CI (confidence intervals) for the EC₅₀ values were calculated by fitting all rounds from each laboratory with a Bayesian statistical model. The asymmetric uncertainty is shown for the median value. The consensus values were generated by using all the interlaboratory data in a Bayesian statistical model.

² outlier not included in the determination of the consensus value.



Tab. S6: Delivered doses at 24 h and 48 h in the absence and presence of serum, respectively, expressed in terms of the fraction delivered, and the number, surface area (of a sphere) and mass dose per cm² well bottom in terms of primary NPs for an administered dose of $c_{adm} = 100 \mu\text{g/ml}$

	Fraction delivered	Number dose (#/cm ²)	Surface area dose (cm ² NPs /cm ²) ¹	Mass dose ($\mu\text{g/cm}^2$)
RPMI - 24 h, $d_H = 56 \text{ nm}$	0.1942	1.18E+11	11.65	11.42
RPMI - 24 h, $d_H = 62 \text{ nm}$	0.1846	1.12E+11	11.08	10.86
RPMI - 24 h, $d_H = 68 \text{ nm}$	0.1764	1.07E+11	10.59	10.37
RPMI/10% FBS - 48 h, $d_H = 1094 \text{ nm}$	0.0686	4.18E+10	4.12	4.04
RPMI/10% FBS - 48 h, $d_H = 1214 \text{ nm}$	0.0662	4.04E+10	3.98	3.90
RPMI/10% FBS - 48 h, $d_H = 1334 \text{ nm}$	0.0643	3.91E+10	3.86	3.78

¹ The surface area dose is defined as the surface area of a sphere per cm² well bottom, in terms of primary NP size. To obtain the number of deposited monolayers, this value can be divided by 4 (assuming full packing, 100% surface coverage) or 8 (assuming random close packing, 50% coverage).


Tab. S7: Dosimetrically corrected mean EC₅₀ values for d_H = 62 nm (RPMI) and d_H = 1214 nm (RPMI/10% FBS)

	mean EC ₅₀ (µg/ml)	corrected EC ₅₀ number dose (#/cm ²)		corrected EC ₅₀ SA dose (cm ² NPs/cm ²)		corrected EC ₅₀ mass dose (µg/cm ²)	
		24 h	48 h	24 h	48 h	24 h	48 h
A549-A cells, serum-free							
Consensus	22.5	2.53E+10	–	2.49	–	2.44	–
Lab A	10.4	1.17E+10	–	1.15	–	1.13	–
Lab B	21.1	2.37E+10	–	2.34	–	2.29	–
Lab C	21.2	2.38E+10	–	2.35	–	2.30	–
Lab D	25.1	2.82E+10	–	2.78	–	2.73	–
A549-B cells, serum-free							
Consensus	22.1	2.49E+10	–	2.45	–	2.40	–
Lab A	22.6	2.54E+10	–	2.50	–	2.45	–
Lab B	23.6	2.65E+10	–	2.62	–	2.56	–
Lab C	23.3	2.62E+10	–	2.58	–	2.53	–
Lab D	25.8	2.90E+10	–	2.86	–	2.80	–
Lab E	15.3	1.72E+10	–	1.70	–	1.66	–
A549-A cells, with serum							
Consensus	57.7	–	2.33E+10	–	2.29	–	2.25
Lab A	52.2	–	2.11E+10	–	2.08	–	2.03
Lab B	52.8	–	2.13E+10	–	2.10	–	2.06
Lab C	61.6	–	2.49E+10	–	2.45	–	2.40
Lab D	64.1	–	2.59E+10	–	2.55	–	2.50
A549-B cells, with serum							
Consensus	52.6	–	2.12E+10	–	2.09	–	2.05
Lab A	47.6	–	1.92E+10	–	1.89	–	1.85
Lab B	49.7	–	2.01E+10	–	1.98	–	1.94
Lab C	62.7	–	2.53E+10	–	2.49	–	2.44
Lab D	56.1	–	2.26E+10	–	2.23	–	2.19
Lab E	47.2	–	1.90E+10	–	1.88	–	1.84

Variations in d_H (±10%) introduce variabilities of +5.17% (d_H = 56 nm) and -4.47% (d_H = 68 nm) in serum-free conditions (RPMI) as well as +3.61% (d_H = 1094 nm) and -3.00% (d_H = 1334 nm) in the presence of serum (RPMI/10% FBS). The difference in variability is not equal because size and particle transport do not correlate linearly.

**Tab. S8: ISDD model input parameters for the MTS assay in serum and serum-free treatments**

Values for media viscosity and density are taken from literature (DeLoid et al., 2014; Hinderliter et al., 2010).

	RPMI	RPMI/10% FBS
1) primary NP properties		
1a) diameter (nm)	56	56
1b) density (g/ml)	1.05	1.05
2) NP agglomerate properties		
2a) diameter (nm)	62 ±6	1214 ±120
2b) density (g/ml)	NA	0.03022
2c) fractal dimension	2.3	2.3
2d) packing factor	0.637	0.637
3) exposure medium properties		
3a) dish depth (m)	0.00588	0.00588
3b) volume (ml)	0.2	0.2
3c) temperature (K)	310	310
3d) viscosity (Ns/m ²)	0.00069	0.00074
3e) density (g/ml)	1.0072	1.0084
3f) exposure time (h)	24 h	48 h

**Tab. S9: EC₅₀ values for CdSO₄ in A549-A and A549-B cells in the absence or presence of serum**

	Mean (μmol/l) ¹	Median (μmol/l)	95% CI (lower limit, upper limit) (μmol/l)
<i>A549-A cells – serum-free</i>			
Consensus	24.9	24.9	22.7, 27.0
Lab A ²	24.4	24.5	23.1, 25.0
Lab B	24.9	25.0	23.9, 26.0
Lab C	24.0	24.2	21.7, 25.0
Lab D	26.2	25.9	25.1, 29.2
<i>A549-B cells – serum-free</i>			
Consensus	49.7	49.9	47.5, 51.5
Lab A	25.6	25.5	25.0, 26.9
Lab B	50.0	49.9	48.0, 51.2
Lab C	50.1	50.0	48.9, 51.7
Lab D	50.0	49.9	48.5, 51.2
Lab E	49.3	49.9	43.9, 50.9
<i>A549-A cells – with serum</i>			
Consensus	58.8	56.2	50.5, 82.5
Lab A	59.7	56.2	50.6, 88.5
Lab B	55.6	55.2	50.6, 65.2
Lab C	59.6	56.2	50.6, 88.8
Lab D	59.7	56.0	50.6, 91.0
<i>A549-B cells – with serum</i>			
Consensus	77.0	77.2	54.3, 99.4
Lab A	76.0	74.4	53.8, 99.3
Lab B	76.0	74.2	53.7, 99.3
Lab C	76.8	75.2	53.8, 100.2
Lab D	75.7	73.6	53.3, 99.3
Lab E	76.1	74.5	53.8, 99.3

¹ The mean, median, and 95% confidence intervals for the EC₅₀ values were calculated by fitting all rounds from each laboratory with a Bayesian statistical model. The asymmetric uncertainty is shown for the median value. The consensus values were generated by using all the interlaboratory data in a Bayesian statistical model.

² Outlier not included in the determination of the consensus value.

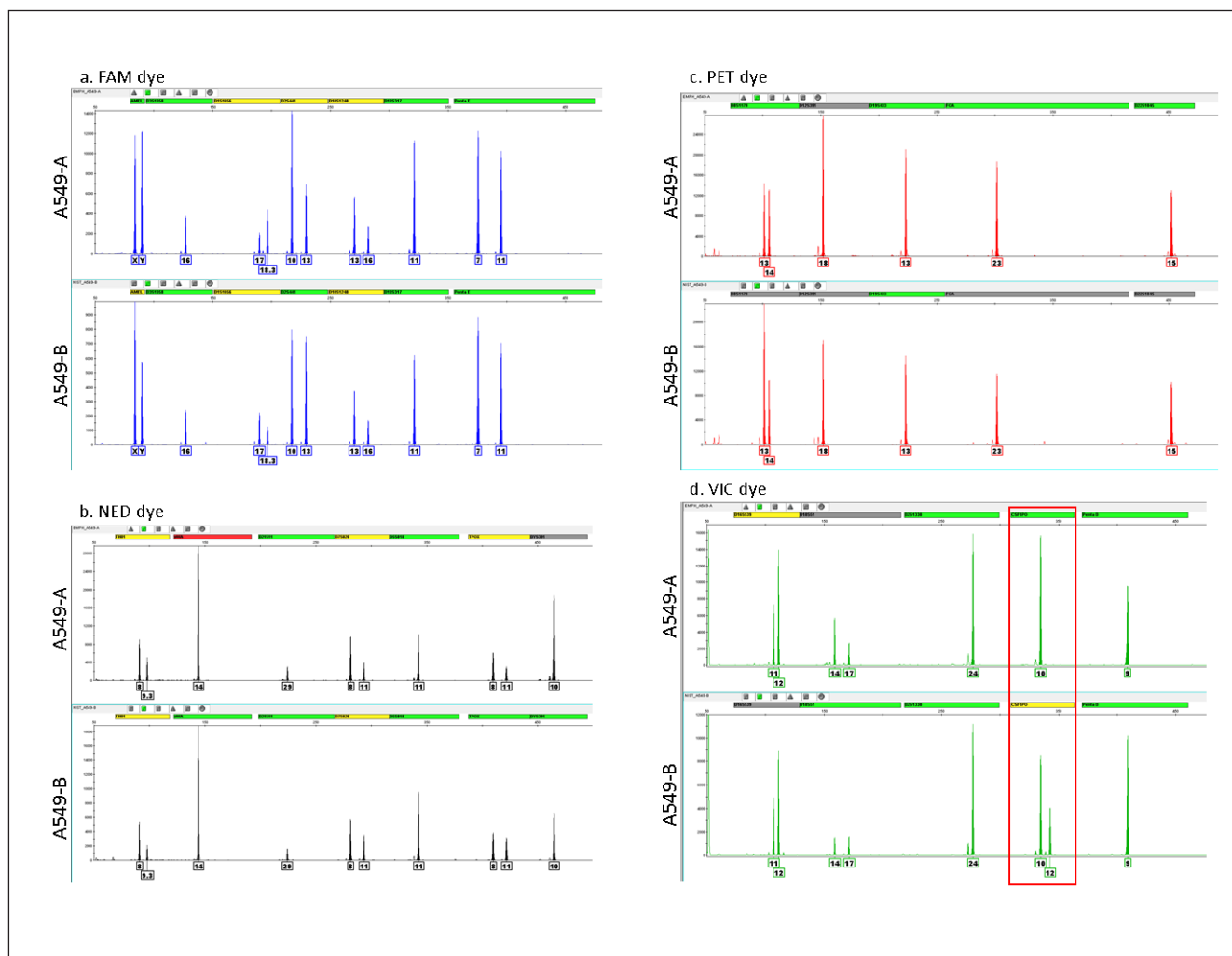


Fig. S1: A549 Cell Line Authentication by Short Tandem Repeat DNA sequences for cell lines A549-A and A549-B

Both cell lines were authenticated and compared by their STR genotypes (PowerPlex Fusion, Promega, Madison, WI). The results indicate that the A549-B cells have the expected STR markers as described by the vendor (ATCC, Manassas, VA). Interestingly, the A549-A cells have 23 identical STR markers with the exception of a single drop out of the 12 allele at the CSF1PO locus (VIC Dye Channel, Fig. S3d). This locus is located on chromosome 5 and suggests that A549-A cell line may have a mutation in the primer binding site, which may have caused failure in the amplification of the 12 allele.

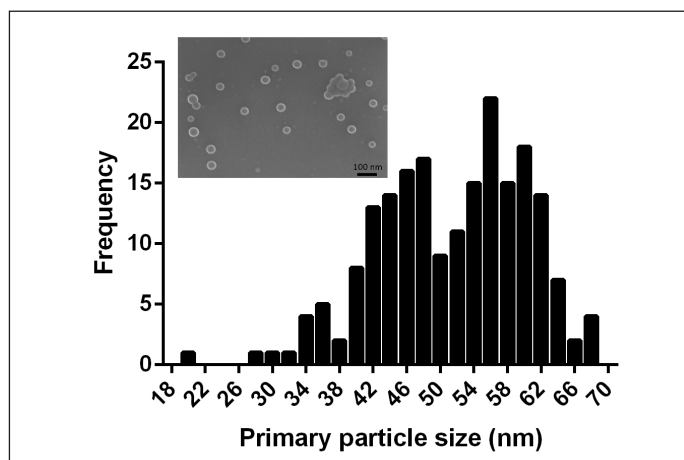


Fig. S2: Scanning electron micrograph and primary particle size histogram for the NH₂-PS NP

Reprinted with permission of The Royal Society of Chemistry (Hanna et al., 2016).



C References

- Cohen, J., DeLoid, G., Pyrgiotakis, G. et al. (2012). Interactions of engineered nanomaterials in physiological media and implications for in vitro dosimetry. *Nanotoxicology* 7, 417-431.
- DeLoid, G., Cohen, J. M., Darrah, T. et al. (2014). Estimating the effective density of engineered nanomaterials for in vitro dosimetry. *Nat Commun* 5, 10. <https://doi.org/10.1038/ncomms4514>
- DeLoid, G. M., Cohen, J. M., Pyrgiotakis, G. et al. (2015). Advanced computational modeling for in vitro nanomaterial dosimetry. *Part Fibre Toxicol* 12, 1.
- Hanna, S. K., Cooksey, G. A., Dong, S. et al. (2016). Feasibility of using a standardized *Caenorhabditis elegans* toxicity test to assess nanomaterial toxicity. *Environ Sci: Nano*, in press.
- Hinderliter, P., Minard, K., Orr, G. et al. (2010). ISDD: A computational model of particle sedimentation, diffusion and target cell dosimetry for in vitro toxicity studies. *Part Fibre Toxicol* 7, 36.
- Sterling, M. C., Bonner, J. S., Ernest, A. N. et al. (2005). Application of fractal flocculation and vertical transport model to aquatic sol-sediment systems. *Water Res* 39, 1818-1830.
- Teeguarden, J. G., Hinderliter, P. M., Orr, G. et al. (2007). Particokinetics in vitro: Dosimetry considerations for in vitro nanoparticle toxicity assessments. *Toxicol Sci* 95, 300-312. <https://doi.org/10.1093/toxsci/kfl165>
- Zook, J. M., MacCuspie, R. I., Locascio, L. E. et al. (2011). Stable nanoparticle aggregates/agglomerates of different sizes and the effect of their size on hemolytic cytotoxicity. *Nanotoxicology* 5, 517-530. <https://doi.org/10.3109/17435390.2010.536615>